THE ANATOLIAN JOURNAL OF CARDIOLOGY

Official journal of the TURKISH SOCIETY OF CARDIOLOGY

Is It Time to Pay Attention to Right and Left Ventricular Apical Angles as Clinically Relevant Computed Tomography Measures in Acute Pulmonary Embolism?

ABSTRACT

Background: In acute pulmonary embolism (PE), abrupt right ventricular (RV) pressure overload and ventricular interdependence are primary determinants of hemodynamic deterioration and short-term mortality. Conventional computed tomographic pulmonary angiography (CTPA) markers, such as the RV/left ventricular (LV) diameter ratio, exhibit variable prognostic performance and may not fully capture early geometric remodeling. It was hypothesized that CTPA-derived apical angle metrics, reflecting biventricular geometric distortion, provide complementary prognostic information beyond established clinical scores.

Methods: In this retrospective study of 535 consecutive patients with acute PE, novel CTPA-derived apical geometry metrics were evaluated: the RV apical angle (α_1), the LV apical angle (α_2), and their ratio (α_1/α_2). The primary outcome was in-hospital mortality; long-term all-cause mortality served as the secondary outcome.

Results: Higher α_1 and α_1/α_2 values were significantly associated with greater pulmonary arterial obstruction, severe RV dysfunction, and higher clinical risk status. In-hospital mortality increased significantly across α_1 tertiles ($P = .017$). In multiple logistic regression models, after adjustment for the Pulmonary Embolism Severity Index (PESI) score and the conventional RV/LV diameter ratio, both α_1 and α_1/α_2 remained independently associated with in-hospital mortality. Adding these apical metrics to the PESI-based baseline model significantly improved prognostic accuracy, demonstrating substantial incremental value for short-term risk stratification. Mortality risk increased linearly beyond thresholds of $\alpha_1 > 32.5°$ and $\alpha_1/\alpha_2 > 1.17$. In multiple Cox proportional hazards analysis, no imaging-derived parameter independently predicted long-term mortality.

Conclusions: Computed tomographic pulmonary angiography–derived apical angle metrics provide physiologically meaningful, continuous measures of acute RV geometric remodeling in acute PE. These metrics offer significant incremental prognostic value for in-hospital mortality beyond the PESI score and conventional CT markers.

Keywords: Apical angle, computed tomography, pulmonary embolism, right ventricle

INTRODUCTION

Acute pulmonary embolism (PE) is a life-threatening condition in which an abrupt increase in right ventricular (RV) afterload is a key driver of early clinical deterioration and short-term mortality.[1-7] The adaptive capacity of the RV to tolerate this sudden pressure overload by occluded pulmonary artery (PA) largely determines hemodynamic stability and early prognosis in acute PE.[1-4,8-20] Accordingly, currently available PE guidelines highlighted an integrated risk-stratification strategy that combines clinical and hemodynamic risk status, biomarkers of myocardial injury, and imaging findings.[1-3] Using this updated risk algorithm of European Society of Cardiology (ESC) /European Respiratory Society (ERS) 2019 PE Guidelines, the overall acute PE spectrum has been classified into 4 risk groups as high-risk, intermediate-to-high-risk, intermediate-to-low-risk, and low-risk status.[3]

In this context, computed tomographic pulmonary angiogram (CTPA) represents a pivotal position from diagnosis to initial risk stratification and monitoring the

ORIGINAL INVESTIGATION

Barkın Kültürsay[1]
Cihangir Kaymaz[2]
Yiğit Cengiz Erkuş[3]
Bahadir Erdem Öcal[4]
Seda Tanyeri Üzel[5]
Hacer Ceren Tokgöz[5]
Çağlar Emre Çağlıyan[6]
Berhan Keskin[7]
Çağdaş Buluş[5]
Doğan Şen[5]
İpek Akkuş[5]
Azmican Kaya[5]
Oğuz Dönmez[5]
Ömer Doğukan Ertan[5]
Muhammet Bulut[5]
Aykun Hakgör[7]
Şeyhmus Külahçıoğlu[5]
Nihal Özdemir[5]

[1]*Department of Cardiology, Tunceli State Hospital, Tunceli, Türkiye*
[2]*Department of Cardiology, Faculty of Medicine, Başkent University, İstanbul, Türkiye*
[3]*Department of Pediatrics, University of Wisconsin-Madison School of Medicine and Public Health, Wisconsin, United States*
[4]*Department of Nuclear Medicine, Faculty of Medicine, İstanbul University Cerrahpaşa, İstanbul, Türkiye*
[5]*Department of Cardiology, Kartal Koşuyolu Heart Training and Research Hospital, İstanbul, Türkiye*
[6]*Department of Cardiology, Faculty of Medicine, Çukurova University, Adana, Türkiye*
[7]*Department of Cardiology, Faculty of Medicine, Medipol University, İstanbul, Türkiye*

Corresponding author:
Cihangir Kaymaz,
✉ cihangirkaymaz2002@yahoo.com

Received Date: March 16, 2026
Accepted Date: July 24, 2026
Available Online Date: September 21, 2026

Cite this article as: Kültürsay B, Kaymaz C, Erkuş YC, et al. Is it time to pay attention to right and left ventricular apical angles as clinically relevant computed tomography measures in acute pulmonary embolism? *Anatol J Cardiol.* 2026;XX(X):X-X.

DOI: 10.14744/AnatolJCardiol.2026.6458

resolution of thrombo-obstructive burden in PA and recovery of RV function.[1-3,6-14] In daily clinical practice, RV-to-left ventricular (LV) diameter ratio (RV/LV ratio), interventricular septal (IVS) flattening, PA diameters, right atrial enlargement, and contrast reflux into the dilated inferior vena cava have been used as surrogates for RV response to acute pressure burden.[1-3,6-14] However, large meta-analyses and comparative studies have shown that the prognostic performance of these CTPA markers, particularly the RV/LV diameter ratio, suffers from important variabilities, and their sensitivity for RV pressure strain is limited at the earlier phase of acute PE.[1-3,6-14] These findings suggest that unidimensional measurements alone may not fully capture the complex geometric consequences of acute RV afterload mismatch leading to lateral expansion of the RV free wall and leftward displacement of the IVS, resulting in characteristic alterations in RV and LV geometry because of the ventricular interdependence.[6-11] Therefore, imaging metrics that reflect these geometric changes as continuous relations may provide a more sensitive representation of RV stress than binary or threshold-based dichotomized measures. Furthermore, other parameters obtained from echocardiography such as tricuspid regurgitation (TR) grade, tricuspid annular planar systolic excursion (TAPSE), and tissue Doppler systolic velocity (S′), strain and strain rate analyses of RV myocardium, 3-dimensional volumetric and functional measures, systolic PA pressure estimates (PASP), and TAPSE/PASP ratio as an index for RV–PA coupling status have been shown to provide additional prognostic information in this setting.[15-26]

Quantitative assessment of the reciprocal changes in RV and LV geometry at the apical level has emerged as a promising concept. On axial CTPA images, changes in the angular relationship between the RV free wall and the IVS directly reflect septal deviation and RV cavity distortion under acute pressure strain.[23] This approach allows simultaneous assessment of the remodeling in RV and LV cavities sharing the same IVS and apex.

In this study, 2 novel CTPA-derived measures of RV apical geometry were proposed: the apical angles formed between the IVS and the free walls of the RV and LV (α_1 and α_2), as well as their ratio (α_1/α_2). This study aimed to investigate whether these continuous metrics are associated with clinical and hemodynamic severity, PA obstruction burden, imaging markers of RV dysfunction, and in-hospital and long-term outcomes in patients with acute PE. In addition, the potential incremental value of these metrics for risk stratification was evaluated when integrated with the Pulmonary Embolism Severity Index (PESI) and the RV/LV diameter ratio.

HIGHLIGHTS

- Computed tomographic pulmonary angiography–derived apical angles (α_1 and α_2) quantify right ventricle (RV) geometric remodeling in acute pulmonary embolism.
- Higher α_1 and α_1/α_2 values reflect greater pulmonary artery obstruction and RV dysfunction
- Apical angle metrics are associated with higher in-hospital mortality
- α_1 and α_1/α_2 add prognostic information beyond Pulmonary Embolism Severity Index for in-hospital risk.

METHODS

Study Design, Patient Population, and Risk Stratification

This study was designed as a retrospective, observational analysis to investigate the prognostic value of the α_1 and α_2 and the α_1/α_2 ratio in consecutive patients with a confirmed diagnosis of acute PE between October 2012 and April 2024. The study protocol was reviewed and approved by the Institutional Clinical Research Ethics Committee of the participating institution (Approval no: 2026/05/1399, Date: October 3, 2026). Owing to the retrospective design and the use of anonymized data, the requirement for informed consent was waived. The study was conducted in accordance with the principles of the Declaration of Helsinki.

The diagnosis of acute PE and risk stratification algorithms have been based on clinical assessment, laboratory findings, and contrast-enhanced multidetector CTPA established in accordance with the criteria defined in the 2014 and 2019 ESC/ERS PE guidelines depending on the time of admission to the Institution.[1-3]

A total of 955 patients diagnosed with acute PE were screened for eligibility. Inclusion criteria were as follows: (i) a confirmed diagnosis of acute PE according to ESC/ERS guideline definitions; (ii) availability of contrast-enhanced CTPA performed at presentation; and (iii) complete clinical, laboratory, and imaging data set, including the PESI and the simplified PESI (sPESI) risk scores, cardiac biomarkers, and transthoracic echocardiographic assessment.[1-4] Exclusion criteria were as follows: symptom onset exceeded 14 days prior to presentation, need for emergency surgical embolectomy because of hemodynamic instability, insufficient CTPA image quality precluding reliable measurements, a known history of severe valvular or congenital heart diseases, or incomplete follow-up data. Using these criteria, 535 out of the 955 patients in whom apical angles (α_1 and α_2) measurements were feasible and who fulfilled all eligibility criteria constituted the final study population.

Treatment strategies were selected according to risk-based treatment algorithms that consider individual clinical risk status, age, comorbid conditions, bleeding risk, and absolute or relative contraindications. The therapeutic approaches used included anticoagulant therapy, systemic thrombolytic therapy (TT) with intravenous tissue-type plasminogen activator, ultrasound-assisted catheter-directed thrombolysis (USAT), AngioJet rheolytic thrombectomy (RT), or combinations of these modalities. In all patients, intravenous unfractionated heparin was initiated as first-line therapy, with the activated partial thromboplastin time targeted between 50 and 75 seconds. Following clinical stabilization, eligible patients were transitioned to low-molecular-weight heparin or oral anticoagulant therapy, as appropriate.

Computed Tomographic Pulmonary Angiography and Imaging Measurements

All CTPA examinations were performed using multidetector helical CT systems according to standardized acquisition protocols. Typical imaging parameters included a tube voltage of 120 kV, automatic tube current modulation (mAs), 0.5-0.6 mm collimation, a pitch of 1.0-1.2, and a reconstructed slice thickness of 1 mm. Contrast material (80-100 mL of non-ionic iodinated contrast) was administered at a rate of 4 mL/s using an automatic bolus-tracking technique with the region of interest placed at the level of the main PA.

All CT measurements were performed by a single experienced observer blinded to clinical data and outcomes, using a predefined and standardized measurement protocol to ensure internal consistency. Since CTPA examinations were primarily performed under emergency settings, the tomographic acquisitions were conducted without electrocardiogram (ECG)-gated synchronization. Therefore, end-diastole was consistently approximated by identifying the specific axial section where the maximal ventricular dimensions were captured. The following measurements were obtained from CTPA images: PA obstruction burden according to the Qanadli score (QS), end-diastolic RV/LV diameter ratio and right atrium (RA) to left atrium (RA/LA) diameter ratio, RV long-axis dimension from tricuspid annulus to apex, apical angles (α_1 and α_2), α_1/α_2 ratio, and diameters of the main, right, and left PA measured on axial images. The presence of pulmonary infarction was defined as peripheral, wedge-shaped consolidation in hypoperfused lung segments.

A schematic illustration of the measurement technique and representative examples is shown in Figure 1, and the protocol is given in Supplementary Material. The α_1 angle was defined as the angle formed by 2 lines drawn from the RV apex to the medial and lateral edges of the tricuspid annulus—one following the most prominent contour of the interventricular septum on the RV side and the other along the lateral contour of the RV free wall (Figure 1). To obtain this measurement, the axial CT slice demonstrating the maximal RV cavity dimension was first identified, and the angle between the 2 lines was measured in degrees.

The α_2 angle was measured in an analogous manner as the angle between 2 lines drawn from the LV apex to the medial and lateral edges of the mitral annulus. The α_1/α_2 ratio was used as a dimensionless index reflecting the relative degree of RV geometric remodeling in comparison with LV geometry.

To assess the reproducibility and clinical reliability of the proposed CTPA metrics, an inter-observer variability analysis

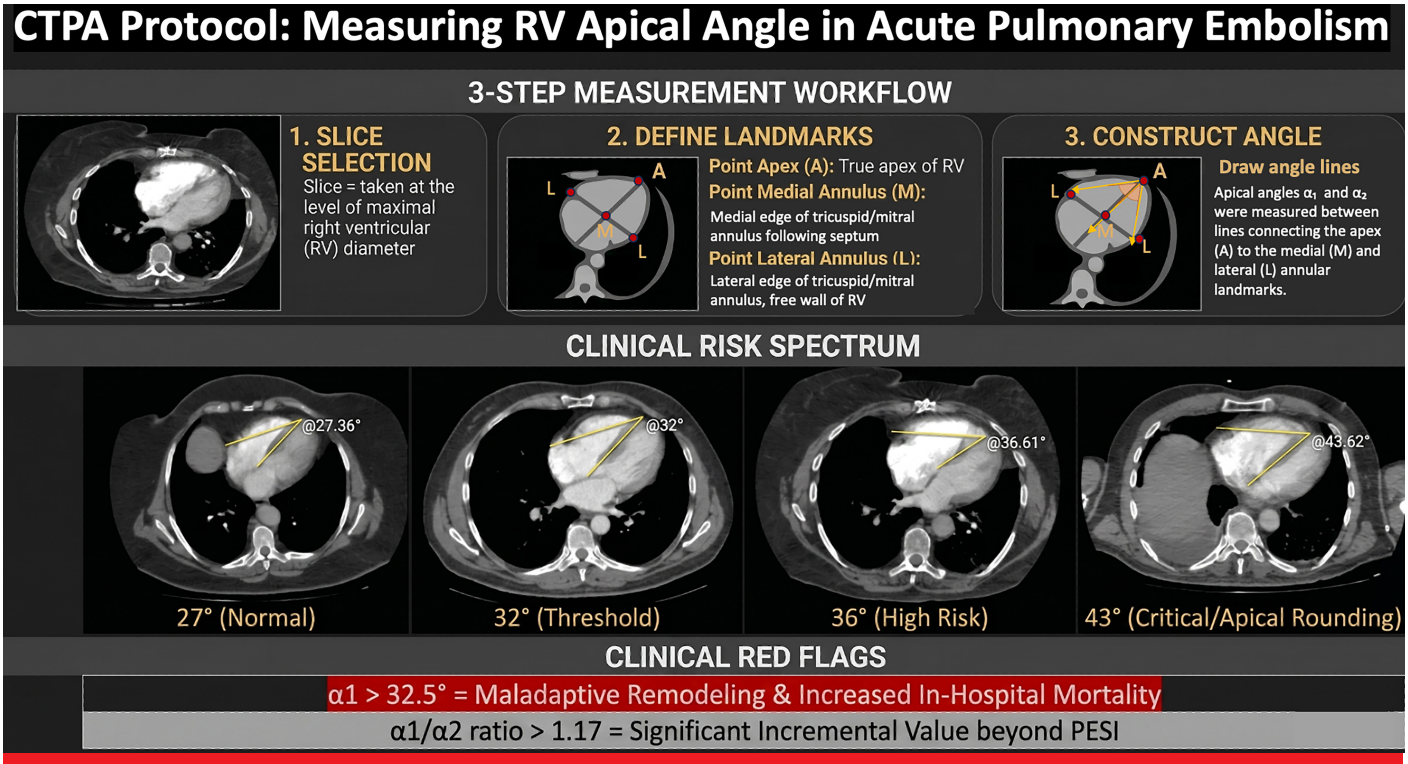

Figure 1. Standardized measurement protocol for ventricular apical angles and clinical risk stratification in acute pulmonary embolism. The top panel illustrates the 3-step measurement workflow: (1) selection of the CT slice at the level of maximal right ventricular (RV) diameter; (2) definition of anatomical landmarks, including the true apex (A), medial annulus (M), and lateral annulus (L); and (3) construction of apical angles α_1 (RV) and α_2 (LV) by connecting the apex to the respective annular edges. The middle panel demonstrates the clinical risk spectrum, where increasing apical angles reflect progressive maladaptive remodeling, ranging from a normal configuration 27° to critical apical rounding 43°. The bottom panel highlights key clinical "red flags," identifying an $\alpha_1 > 32.5°$ as a predictor of increased in-hospital mortality and an α_1/α_2 ratio > 1.17 as providing significant incremental prognostic value beyond the Pulmonary Embolism Severity Index (PESI).

was performed. After the initial measurements, a second independent observer, blinded to the clinical outcomes and the first observer's results, re-evaluated α_1 and α_1/α_2 in a randomly selected subset of 50 patients (approximately 10% of the total cohort). Inter-observer reliability was quantified using the 2-way random-effects model, absolute agreement, single-rater Intraclass Correlation Coefficient (ICC). Additionally, Bland–Altman analysis was conducted to evaluate the presence of any systematic bias between the 2 observers.

Echocardiography

Transthoracic echocardiography was performed in all patients within the first 24 hours after admission and repeated before discharge. Examinations were conducted in accordance with the recommendations of the American Society of Echocardiography (ASE) and the European Association of Cardiovascular Imaging (EACVI).[15-17] From parasternal and apical views, the following parameters were assessed: RV and LV end-diastolic diameters, RA planimetric area, TAPSE, S′, and PASP estimated from TR jet, and the TAPSE/PASP ratio as a non-invasive surrogate for RV–PA coupling.[1-3,15-21,25,26]

Outcome Definitions

The primary outcome of the study was defined as all-cause mortality occurring during the index hospitalization. Secondary (exploratory) outcomes included long-term all-cause mortality. Long-term mortality was defined as death from any cause occurring between the date of initial presentation and the date of death or the last available follow-up. Safety outcomes included the occurrence of major and minor bleeding events. Major bleeding was defined according to the criteria of the International Society on Thrombosis and Hemostasis (ISTH) as clinically overt bleeding associated with a decrease in hemoglobin level of $\geq$2 g/dL, the need for transfusion of at least 2 units of red blood cells, or bleeding at a critical site (including intracranial, intraspinal, intraocular, pericardial, intrathoracic, intra-abdominal, or retroperitoneal bleeding).[27] Clinically evident bleeding events that did not meet these criteria were classified as minor bleeding.

Statistical Analysis

Continuous variables are presented as mean ± SD or median (interquartile range), as appropriate, while categorical variables are summarized as counts and percentages. The normality of continuous variables was evaluated using the Kolmogorov–Smirnov test for the overall cohort and the Shapiro–Wilk test for subgroup analyses, supplemented by visually inspected Q–Q plots. Patients were categorized into tertiles based on the α_1 to evaluate the distribution of baseline characteristics and clinical variables across groups. Between-group comparisons were performed using one-way analysis of variance (ANOVA) or Kruskal–Wallis tests for continuous variables, and chi-square or Fisher's exact tests for categorical variables, as appropriate.

Logistic regression analyses were performed to identify factors associated with the primary outcome (in-hospital mortality). Odds ratios (ORs) and 95% CIs were reported for each 1-degree increase in α_1 and for each 1% increase in the α_1/α_2 ratio. To reduce the risk of overfitting, the PESI score was used as the core clinical covariate in multiple regression models. Separate models were constructed by adding either α_1 or the α_1/α_2 ratio to PESI to evaluate their incremental prognostic contribution. In sensitivity analyses, the RV/LV diameter ratio was additionally included in the models. Potential non-linear associations between α_1, the α_1/α_2 ratio, and mortality were explored using restricted cubic spline functions with 3 knots. Linear and non-linear components were compared using Wald tests. Predicted probabilities of in-hospital mortality across observed ranges of α_1 and α_1/α_2 were estimated while holding PESI constant, and the resulting curves were graphically displayed. Discriminative performance was assessed using receiver operating characteristic (ROC) curve analysis, with calculation of the area under the curve (AUC) for α_1 and the α_1/α_2 ratio. To address potential overfitting and ensure model stability, internal validation was performed using a bootstrap resampling procedure (1000 iterations). Long-term mortality was analyzed using Cox proportional hazards regression models, with time from index presentation to death or last follow-up considered as the time-to-event variable.

All statistical analyses were performed using R software (version 4.3.1; R Foundation for Statistical Computing, Vienna, Austria), employing the rms, pROC, ggplot2, survival, survminer, and dplyr packages. A 2-sided *P* value < .05 was considered statistically significant.

RESULTS

In the 535 patients with hemodynamically stable or unstable acute PE included in the study, the mean α_1 was 31.9°, ranging from 19.3° to 47.1°. According to α_1 values, patients were stratified into low (19.3-29.9°, n = 178), intermediate (29.9-33.3°, n = 178), and high (33.3-47.1°, n = 179) tertiles. Demographic, clinical, and imaging characteristics, treatment patterns, and in-hospital outcomes across α_1 angle tertiles were given in Table 1. The α_1/α_2 ratio increased from approximately 0.97 in the lowest tertile to 1.28 in the highest tertile ($P < .001$). The higher tertile was significantly associated with an older age, a higher frequency of female gender, a longer duration from symptom onset, a higher incidence of hypertension, a lower incidence of smoking history, a lower pulse oximetric saturation, and a higher PESI score and PESI class (Table 1). According to the ESC/ERS risk stratification, the proportion of low-risk patients tended to decrease from 21% to 11% across tertiles, whereas high-risk PE increased from 3.9% to 6.7% ($P = .054$) (Figure 2).

Among CTPA and echocardiographic measures, QS in the main and right PAs, RA area, diameters of the right and left PAs and inferior vena cava, as well as the RV/LV and RA/LA diameter ratios, were significantly higher, and severe TR was more frequent in the highest α_1 tertile (Table 1). Although treatment modalities and hospital stay duration of patients were comparable across the α_1 tertiles, higher tertile was associated with increased risks for major bleeding and in-hospital mortality ($P = .010$ and $P = .017$, respectively). At the time of hospital discharge, TAPSE and S′ velocities were lower, whereas TR grade, PASP, TAPSE/PASP ratio, RV/LV and

Table 1. Clinical, Imaging, and Outcome Profiles Across α_1 Angle Tertiles

Variables	Low (19.33-29.95, n = 178)	Mid (29.86-33.34, n = 178)	High (33.35-47.09, n = 179)	*P*
Demographic and clinical characteristics				
Age (years)	51.4 (17.1)	61.2 (15.4)	64.5 (13.1)	<.001[a, b]
Female, n (%)	77 (43.3)	105 (59)	114 (63.7)	<.001
Syncope (yes/no)	45 (25.3)	50 (28.1)	48 (26.8)	.835
Symptom onset (days)	3 (2-69	3 (2-7)	4 (2-7)	.017[b]
Hypertension, n (%)	46 (25.8)	64 (36)	81 (45.3)	<.001
Coronary artery disease, n (%)	15 (8.4)	14 (7.9)	19 (10.6)	.63
Hyperlipidemia, n (%)	11 (6.2)	13 (7.3)	17 (9.5)	.487
Diabetes mellitus, n (%)	20 (11.2)	36 (20.2)	33 (18.4)	.055
Congestive heart failure, n (%)	2 (1.1)	3 (1.7)	6 (3.4)	.304
Smoking (current smoker), n (%)	37 (20.8)	16 (9)	13 (7.3)	<.001
Chronic obstructive pulmonary disease, n (%)	6 (3.4)	12 (6.7)	7 (3.9)	.27
Immobilization, n (%)	33 (18.5)	33 (18.5)	24 (13.4)	.326
Stroke, n (%)	8 (4.5)	8 (4.5)	8 (4.5)	1
OC/HRT, n (%)	5 (2.8)	1 (0.6)	2 (1.1)	.239
Atrial fibrillation, n (%)	3 (1.7)	10 (5.6)	11 (6.1)	.069
Travel history, n (%)	19 (10.7)	15 (8.4)	7 (3.9)	.052
Acute DVT, n (%)	108 (60.7)	95 (53.4)	87 (46.6)	.07
Past VTE, n (%)	15 (8.4)	19 (10.7)	18 (9.5)	.77
Malignancy, n (%)	20 (11.2)	26 (14.6)	28 (15.6)	.452
Postoperative status, n (%)	37 (20.8)	52 (29.2)	36 (20.1)	.077
Bone fracture, n (%)	12 (6.7)	11 (6.2)	11 (6.1)	.967
Thrombophilia, n (%)	5 (2.8)	0 (0)	0 (0)	.008
Vital signs (initial)				
Systolic BP (mmHg)	126 (22.1)	125 (25)	127 (21.5)	.676
Diastolic BP (mmHg)	77 (15.2)	76.9 (18.8)	78.3 (17.1)	.703
Heart rate (bpm)	108 (18.2)	105 (19.7)	105 (19)	.211
Oxygen saturation (%)	91.5 (88-95)	92 (88-94)	90 (87-93)	.027[b]
PESI score	82 (63-105)	90 (70.3-115)	100 (79-120)	<.001[a, b]
PESI class	2 (1-3)	3 (2-4)	3 (2-4)	<.001[a, b]
sPESI	1 (0-2)	1 (0-2)	1 (1-2)	.505
ESC risk group				.054
Low	38 (21.3)	25 (14)	20 (11.2)	
Intermediate	133 (74.7)	139 (78.1)	147 (82.1)	
High	7 (3.9)	14 (7.9)	12 (6.7)	
Shock index	0.846 (0.729-1.03)	0.828 (0.677-1.05)	0.827 (0.729-0.985)	.493
Modified shock index	0.953 (0.794-1.16)	0.919 (0.733-1.17)	0.913 (0.796-1.13)	.654
Echocardiographic findings				
TR grade				<.001
0	2 (1.1)	0 (0)	0 (0)	
1	61 (34.3)	53 (29.8)	47 (26.3)	
2	85 (47.8)	81 (45.5)	58 (32.4)	
3	22 (12.4)	32 (18)	49 (27.4)	
4	8 (4.5)	12 (6.7)	25 (14)	
D-shaped septum, n (%)	44 (24.7)	52 (29.2)	54 (30.2)	.473
PASP (mmHg)	47.9 (14)	49.9 (13.6)	51.4 (15)	.07
TAPSE (cm)	1.94 (0.43)	1.92 (0.41)	1.87 (0.42)	.22
TAPSE/PASP ratio	0.40 (0.30-0.52)	0.39 (0.28-0.53)	0.36 (0.27-0.47)	.056

(*Continued*)

Table 1. Clinical, Imaging, and Outcome Profiles Across α_1 Angle Tertiles (*Continued*)

Variables	Low (19.33-29.95, n = 178)	Mid (29.86-33.34, n = 178)	High (33.35-47.09, n = 179)	*P*
RV TDI S′ (cm/s)	12.1 (3.01)	11.8 (2.82)	11.2 (2.89)	.161
CT angiography findings				
Qanadli score (Total)	19.5 (14-23.8)	20 (17-24)	20 (16.5-25)	.018[b]
Qanadli score (right lung)	10 (7.75-12.3)	10.5 (9-13)	11 (10-13)	.015[a, b]
Qanadli score (left lung)	10 (5-11)	10 (6-11)	10 (7-12)	.369
RV/LV ratio	1.12 (0.98-1.29))	1.16 (1.02-1.31)	1.20 (1.04-1.36)	.028[b]
RV diameter (mm)	41.7 (8.03)	42.8 (6.21)	43.9 (7.14)	.012[b]
RA/LA ratio	1.18 (0.25)	1.27 (0.3)	1.28 (0.27)	.006[a, b]
MPA diameter (mm)	28.9 (3.92)	29.8 (3.77)	30 (4.49)	.056
LPA diameter (mm)	21.7 (2.81)	22.4 (3.03)	22.7 (2.96)	.016[b]
RPA diameter (mm)	22.3 (3.46)	23.3 (3.19)	23.5 (3.12)	.002[a, b]
MPA/Ao ratio	0.914 (0.82-1.01)	0.871 (0.78-0.98)	0.877 (0.76-0.96)	.095
RV area (cm^2)	2266 (585)	2383 (612)	2352 (668)	.187
RA area (cm^2)	1402 (410)	1619 (494)	1872 (677)	<.001[d]
LV area (cm^2)	2184 (553)	2097 (566)	2056 (656)	.118
LA area (cm^2)	1131 (908-1456)	1280 (974-1604)	1196 (979-1550)	.020[a]
α_1 (degrees)	27 (2.27)	31.6 (0.99)	36.8 (2.78)	<.001[d]
α_2 (degrees)	28.7 (5.59)	29.6 (4.52)	29.5 (4.54)	.189
α_1/α_2 ratio	0.974 (0.19)	1.09 (0.17)	1.28 (0.22)	<.001[d]
Pleural effusion, n (%)	27 (15.2)	22 (12.4)	19 (16.2)	.568
Pulmonary infarction, n (%)	34 (19.1)	31 (17.4)	28 (15.6)	.689
IVC area (cm^2)	517 (148)	540 (141)	564 (185)	.024[b]
RVFWD (mm)	5.21 (1.17)	5.55 (1.75)	5.54 (1.42)	.123
Laboratory values				
D-dimer (μg/mL)	6.51 (3.35-12.3)	5.45 (3.42-10.9)	7.74 (3.69-13.9)	.17
Troponin (ng/L)	0.059 (0.022-0.149)	0.065 (0.028-0.195)	0.071 (0.028-0.198)	.213
CRP (mg/L)	6.27 (2.31-16.2)	3.25 (1.79-10.9)	3.9 (1.9-11.8)	.014[a, b]
Treatments				
USAT (EKOS)	37 (20.8)	43 (24.2)	54 (30.2)	.117
Rheolytic thrombectomy (AngioJet)	17 (9.6)	11 (6.2)	12 (6.7)	.429
tPA (low dose/full dose combined)	58 (32.6)	49 (27.5)	46 (25.7)	.329
Discharge vital, echocardiography and CT findings				
Systolic BP (mmHg)	123 (17.7)	126 (15.9)	124 (14.5)	.192
Diastolic BP (mmHg)	75.6 (9.58)	75.8 (10.9)	75.3 (9.74)	.939
Oxygen saturation (%)	96 (94-97)	96 (94-97)	95 (95-97)	.198
Heart rate (bpm)	83.8 (10.8)	83.6 (11.4)	80.5 (10.8)	.007[b]
Shock index	0.682 (0.613-0.767)	0.654 (0.562-0.75)	0.649 (0.585-0.725)	.061
Modified shock index	0.707 (0.639-0.813)	0.680 (0.583-0.790)	0.677 (0.621-0.764)	.081
TR grade				.002
0	2 (1.7)	0 (0)	2 (1.7)	
1	104 (88.1)	88 (74.6)	79 (65.39	
2	11 (9.3)	26 (22)	29 (24)	
3	1 (0.8)	3 (2.5)	7 (5.8)	
4	0 (0)	1 (0.8)	4 (3.3)	
PASP (mmHg)	33.6 (9.71)	36.3 (11.8)	37.1 (13.3)	.041[b]
TAPSE (cm)	2.38 (0.37)	2.29 (0.38)	2.25 (0.43)	.028[b]
TAPSE/PASP ratio	0.73 (0.6-0.88)	0.66 (0.53-0.83)	0.73 (0.49-0.8)	.003[b]

(*Continued*)

Table 1. Clinical, Imaging, and Outcome Profiles Across α_1 Angle Tertiles (*Continued*)

Variables	Low (19.33-29.95, n = 178)	Mid (29.86-33.34, n = 178)	High (33.35-47.09, n = 179)	*P*
RV TDI S′ (cm/s)	14.5 (2.26)	14.4 (2.39)	13.6 (2.88)	.026[b]
Qanadli score (total)	9 (5-13)	10 (6-15)	9 (5-13)	.183
Qanadli score (right lung)	4 (3-8)	5 (3-9)	5 (2-7.5)	.205
Qanadli score (left lung)	4 (2-6)	4 (2.5-7)	4 (2-6)	.378
RV/LV ratio	0.83 (0.76-0.94)	0.89 (0.82-0.98)	0.92 (0.86-1.01)	<.001[a, b]
RA/LA ratio	0.98 (0.17)	1.02 (0.19)	1.09 (0.2)	<.001[b, c]
MPA (mm)	26.5 (3.63)	27.8 (4.44)	27.6 (4.63)	.035[a]
LPA (mm)	20.1 (2.66)	21.6 (3.66)	21.3 (3.13)	.001[a, b]
RPA (mm)	21 (3.25)	22 (3.41)	22.2 (3.54)	.012[b]
MPA/Ao ratio	0.83 (0.76-0.90)	0.82 (0.75-0.94)	0.80 (0.71-0.90)	.149
Pleural effusion, n (%)	47 (26.5)	45 (25.4)	56 (31.3)	.567
Pulmonary infarction, n (%)	53 (29.9)	45 (25.4)	32 (18.3)	.115
Outcomes				
Major bleeding	1 (0.6)	5 (2.8)	11 (6.1)	.01
Minor bleeding	3 (1.7)	8 (4.5)	12 (6.7)	.051
Hospital stay (days)	9 (7-11)	9 (7-11)	9 (7-13)	.214
In-hospital mortality	1 (0.6)	3 (1.7)	9 (5)	.017

α_1, right ventricular apical angle; α_2, left ventricular apical angle; α_1/α_2, RV/LV apical angle ratio; BP, blood pressure; CRP, C-reactive protein; DVT, deep vein thrombosis; ESC, European Society of Cardiology; IVC, inferior vena cava; LA, left atrium; LA area, left atrial area; LPA, left pulmonary artery; LV, left ventricle; LV area, left ventricular area; MPA, main pulmonary artery; MPA/Ao, main pulmonary artery–to–aorta ratio; OC/HRT, oral contraceptive/hormone replacement therapy; PASP, pulmonary artery systolic pressure; PESI, pulmonary embolism severity index; QS-total, total Qanadli score; QS-right, right lung Qanadli score; QS-left, left lung Qanadli score; RA, right atrium; RA area, right atrial area; RA/LA, right atrium–to–left atrium ratio; RPA, right pulmonary artery; RV, right ventricle; RV area, right ventricular area; RVFWD, right ventricular free-wall diameter; RV/LV, right ventricle–to–left ventricle ratio; SI, shock index; sPESI, simplified pulmonary embolism severity index; TAPSE, tricuspid annular plane systolic excursion; TDI, tissue Doppler imaging; TR, tricuspid regurgitation; tPA, tissue plasminogen activator; USAT, ultrasound-assisted thrombolysis; VTE, venous thromboembolism.
[a]Comparison between low and mid α_1 tertiles (1 vs. 2).
[b]Comparison between low and high α_1 tertiles (1 vs. 3).
[c]Comparison between mid and high α_1 tertiles (2 vs. 3).
[d]Overall comparison among all 3 tertiles.

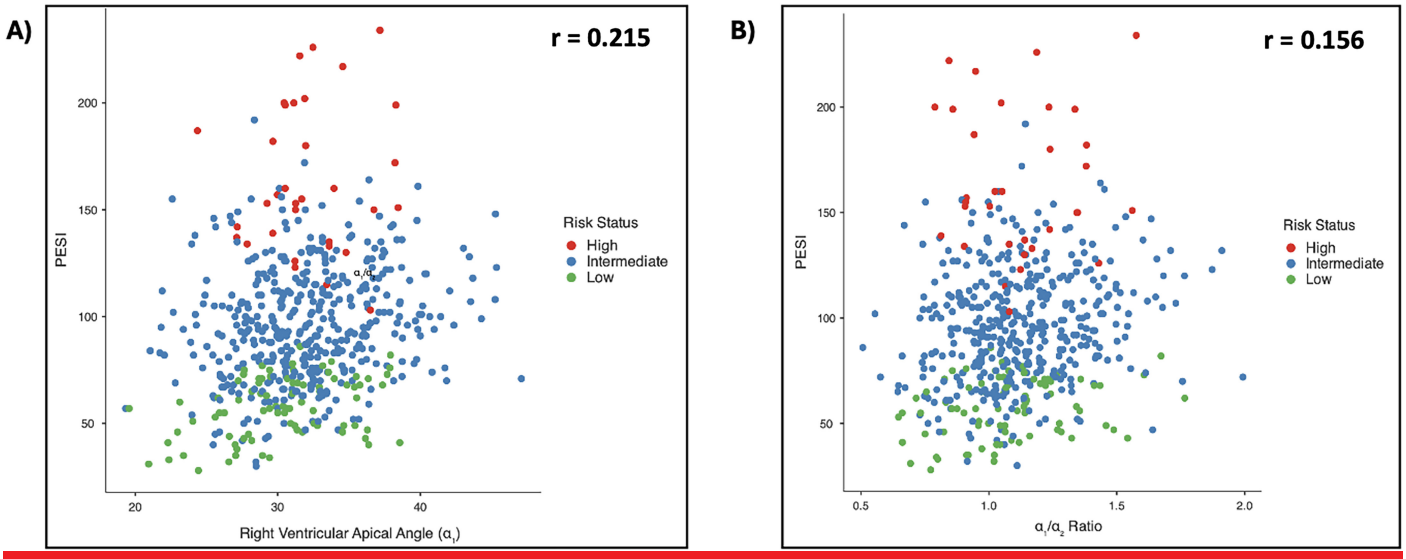

Figure 2. Association of α_1 and the α_1/α_2 ratio with PESI score and ESC risk class. Scatter plots showing the relationships between (A) α_1 (degrees) and PESI score and (B) the α_1/α_2 ratio and PESI score. Each dot represents an individual patient. Colors denote ESC/ERS 2019 risk categories, with low risk shown in green, intermediate risk shown in blue (combining intermediate–low and intermediate–high strata), and high risk shown in red. ESC, European Society of Cardiology; ERS, European Respiratory Society; PESI, Pulmonary Embolism Severity Index.

RA/LA diameter ratios, and PA diameters were higher in the highest α_1 tertile compared with the first 2 tertiles. In contrast, QS values were similar across α_1 tertiles ($P > .05$).

Correlation analyses demonstrated that CTPA-derived apical metrics were significantly associated with echocardiographic markers of RV strain. α_1 showed positive correlations with PASP ($r = 0.199$, $P = .006$) and TR grades ($P < .001$), and an inverse correlation with the TAPSE/PASP ratio ($r = -0.154$, $P = .019$) (Supplementary Figure 3).

Treatment strategies were applied according to risk-based algorithms and did not differ significantly across α_1 tertiles. From the lowest to highest tertiles, USAT was performed in 21%, 24%, and 30% of patients, respectively, while RT was used in 9.6%, 6.2%, and 6.7%. Intravenous t-PA use was comparable across groups, and length of hospital stay was similar between tertiles (median 9 days; $P = .214$).

In contrast, bleeding complications and in-hospital mortality increased with higher α_1 values. Major bleeding occurred in 0.6%, 2.8%, and 6.1% of patients across tertiles ($P = .010$), and minor bleeding in 1.7%, 4.5%, and 6.7% ($P = .051$). In-hospital mortality increased from 0.6% in the lowest tertile to 1.7% and 5.0% in the intermediate and highest tertiles, respectively ($P = .017$).

Optimal cut-off values for predicting in-hospital mortality were determined using the Youden index and were 32.46° for α_1 and 1.17 for the α_1/α_2 ratio. For these cut-off values, the sensitivity, specificity, and AUCs were 85%, 66%, and 0.718 (95% CI: 0.654-0.782, $P < .001$) for α_1, and 77%, 66%, and 0.721 (96% CI: 0.658-0.784, $P < .001$) for the α_1/α_2 ratio, respectively, in predicting in-hospital mortality (Table 2 and Figure 3).

Table 2. ROC-derived Optimal Cut-off Values and Discriminatory Performance of α_1 and the α_1/α_2 Ratio for Predicting In-hospital Mortality

Variables	Cutoff	Sensitivity	Specificity	AUC
α_1 angle (degrees)	32.46	0.85	0.66	0.718
α_1/α_2 ratio (unitless)	1.17	0.77	0.66	0.721

AUC, area under the curve; α_1, right ventricular apical angle; α_2, left ventricular apical angle; α_1/α_2, RV/LV apical angle ratio; ROC, receiver operating characteristic.

In multiple logistic regression analyses, both α_1 and the α_1/α_2 ratio were significantly and independently associated with in-hospital mortality. Each 1° increase in α_1 was associated with increased mortality risk, and this relationship persisted after adjustment for PESI (PESI: [OR = 1.030, $P < .001$, 95% CI: 1.010-1.040]; α_1: [OR = 1.150, $P = .023$, 95% CI: 1.020-1.310] per 1° increase). Similarly, each 10% increase in the α_1/α_2 ratio significantly increased in-hospital mortality risk beyond PESI ($P = .036$). Likewise, adjustment for the RV/LV ratio did not alter the association of α_1 or the α_1/α_2 ratio with in-hospital mortality. In model comparison analyses, the baseline PESI score demonstrated a high discriminative performance for in-hospital mortality (AUC = 0.839). The addition of the α_1

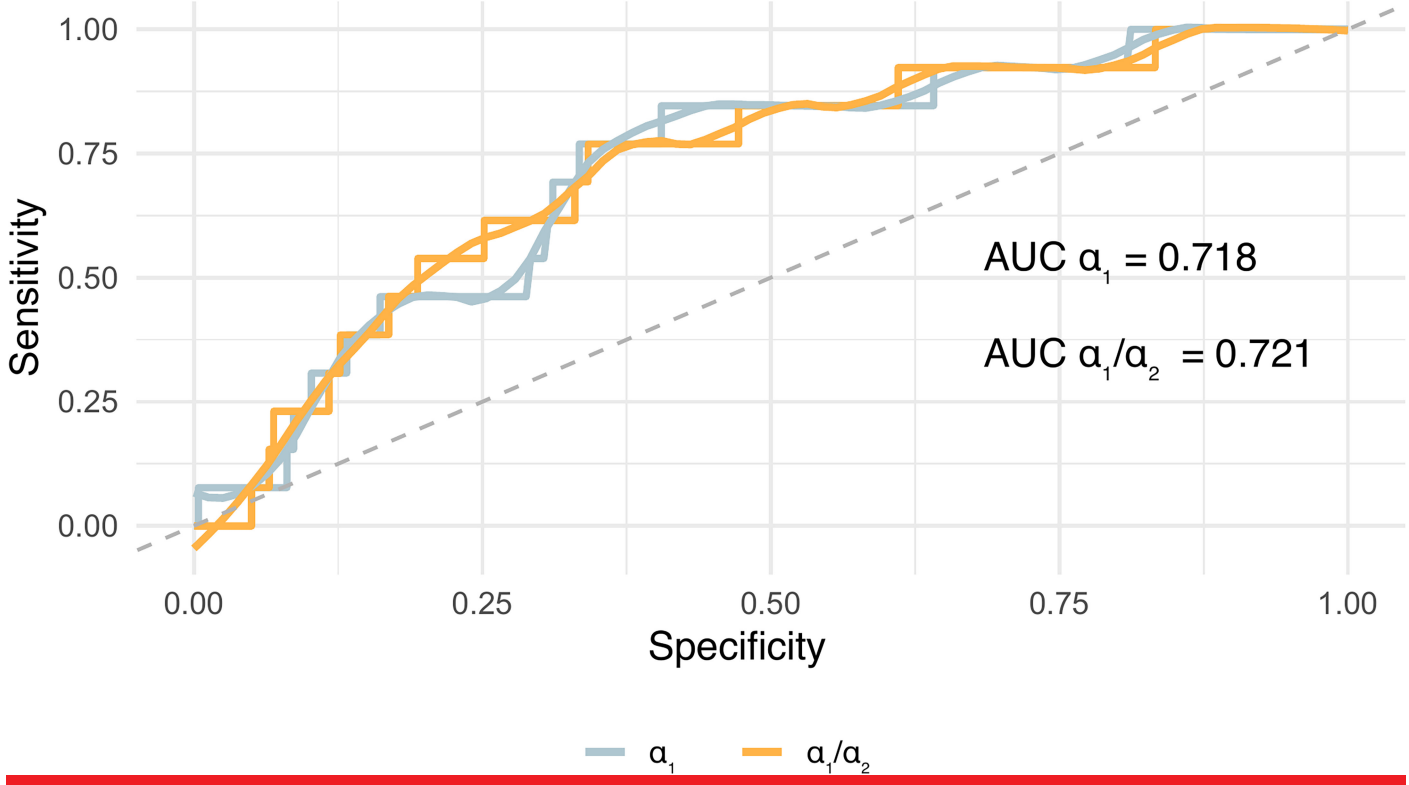

Figure 3. Discriminative performance of α_1 and α_1/α_2 for in-hospital mortality in receiver operating characteristic (ROC) curves depicting the ability of α_1 and the α_1/α_2 ratio to predict in-hospital mortality. The area under the curve (AUC) was 0.718 for α_1 and 0.721 for α_1/α_2. Optimal cut-off values determined by the Youden index were 32.5° for α_1 and 1.17 for α_1/α_2. The dashed diagonal line represents the reference line of no discrimination.

angle (AUC = 0.842) and the α_1/α_2 ratio (AUC = 0.850) to the PESI score resulted in a numerical increase in the discriminative power (Table 3). In the reclassification analysis, the addition of the α_1/α_2 ratio to the PESI-based baseline model significantly improved the prognostic accuracy for in-hospital mortality (continuous net reclassification improvement [NRI] = 0.778, P = .002; integrated discrimination improvement [IDI] = 0.016, P = .034), demonstrating a substantial incremental value over clinical parameters alone (Supplementary Table S1).

Furthermore, sensitivity analyses demonstrated that both α_1 and the α_1/α_2 ratio remained significant independent predictors of in-hospital mortality even after adjusting for the administration of catheter-directed therapies (P = .021 and P = .028, respectively; Supplementary Table S2). Internal validation via bootstrap resampling confirmed the robustness of the integrated model. The original AUC of 0.850 showed minimal optimism (0.004), resulting in an optimism-corrected AUC of 0.847, which suggests acceptable model stability despite the limited event rate.

Restricted cubic spline analyses showed an approximately linear relationship between α_1, α_1/α_2, and in-hospital mortality, with a steeper increase above approximately 30-35° for α_1 and 1.10-1.20 for α_1/α_2 (Figure 4). When PESI was held

Table 3. Multiple Logistic Regression Models for In-hospital Mortality

Model	Predictor	OR (95% CI)	*P*	AUC
PESI		1.032 (1.012-1.044)	<.001	0.839
PESI + α_1	PESI	1.031 (1.011-1.043)	<.001	0.841
	α_1 (per 1°)	1.154 (1.022-1.308)	.023	
PESI + α_1/α_2 ratio	PESI	1.033 (1.013-1.045)	<.001	0.850
	α_1/α_2 ratio (per 10%)	1.082 (1.014-1.153)	.036	
PESI + α_1 + RV/LV ratio	PESI	1.031 (1.011-1.042)	<.001	0.838
	α_1 (per 1°)	1.153 (1.021-1.307)	.027	
	RV/LV ratio	1.442 (0.103-20.412)	.787	
PESI + α_1/α_2 ratio + RV/LV ratio	PESI	1.032 (1.012-1.044)	<.001	0.844
	α_1/α_2 ratio (per 10 %)	1.081 (1.072-1.154)	.043	
	RV/LV ratio	1.463 (0.104-22.115)	.785	

α_1, right ventricular apical angle; α_2, left ventricular apical angle; α_1/α_2, RV/LV apical angle ratio; AUC, area under curve; OR, odds ratio; PESI, pulmonary embolism severity index; RV/LV, right ventricle—to—left ventricle ratio.

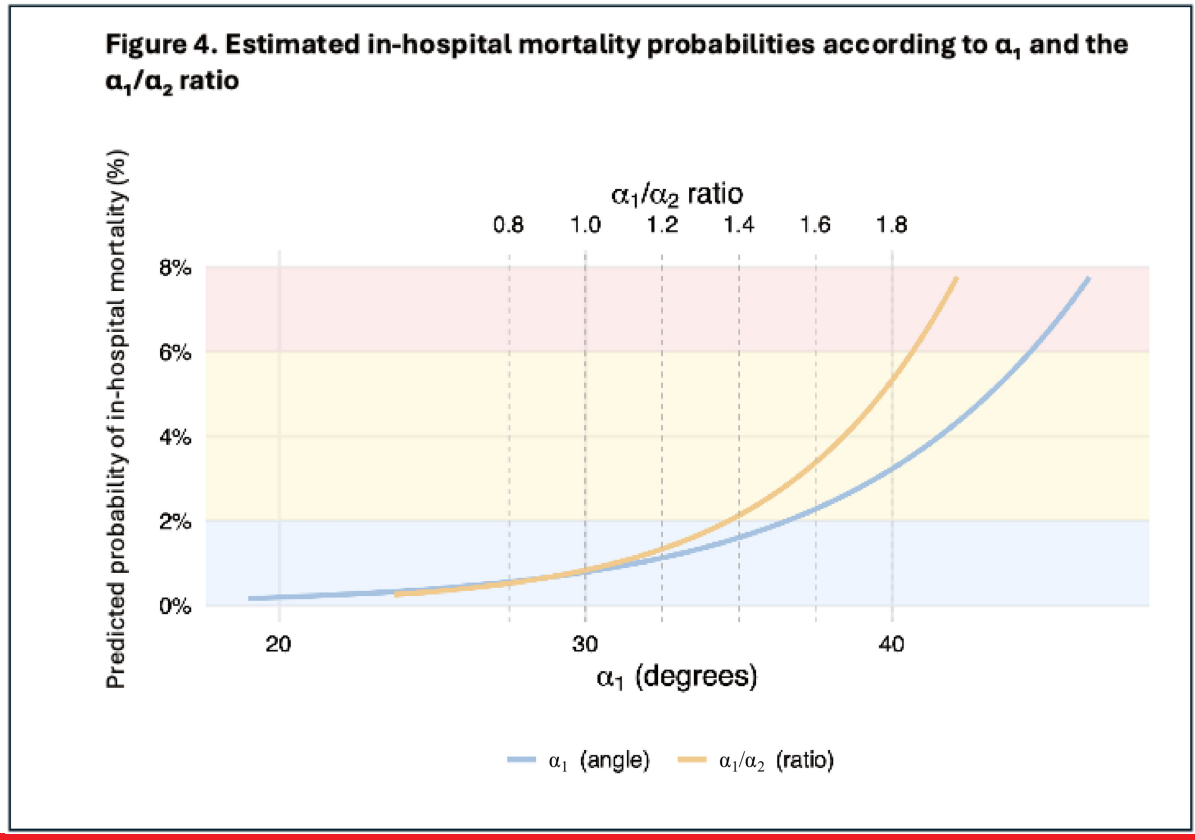

Figure 4. Estimated in-hospital mortality probability according to α_1 and α_1/α_2 (restricted cubic spline models). Restricted cubic spline models adjusted for PESI, illustrating the association between α_1 and α_1/α_2 across their observed ranges and the estimated probability of in-hospital mortality. The risk profile remains relatively flat at lower values, with a more pronounced increase above approximately 30-35° for α_1 and 1.10-1.20 for α_1/α_2. PESI, Pulmonary Embolism Severity Index.

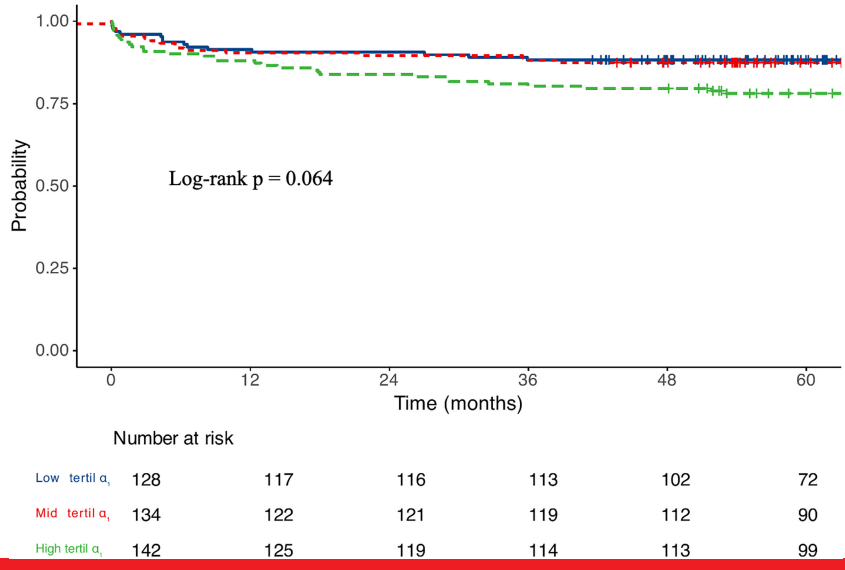

Figure 5. Long-term survival according to α_1 tertiles (Kaplan–Meier analysis). Curves showing long-term all-cause survival stratified by α_1 tertiles: low (green), intermediate (blue), and high (red). The x-axis represents follow-up time (months), and the y-axis indicates survival probability. Numbers at risk are displayed below the x-axis. Group differences were assessed using the log-rank test.

constant, estimated mortality probability increased markedly beyond these thresholds.

The inter-observer reliability analysis demonstrated excellent agreement for both the RV apical angle α_1 and the α_1/α_2 ratio. The ICC was 0.973 (95% CI: 0.952-0.985) for α_1 and 0.970 (95% CI: 0.948-0.983) for the α_1/α_2 ratio. Bland–Altman analysis further confirmed high consistency between the observers, revealing minimal mean biases of −0.07° for α_1 and 0.005 for the α_1/α_2 ratio (Supplementary Figure 1 and 2).

Median follow-up time was 2141 (1589-2695) days. Although Kaplan–Meier analysis showed an initial separation of survival curves across α_1 tertiles, the log-rank test did not reach statistical significance ($P = .064$) (Figure 5).

After adjustment for the PESI score in multiple regression analyses, α_1, TAPSE, and the RV/LV ratio at discharge were not significantly associated with long-term mortality, whereas the PESI score remained associated with the outcome (HR = 1.021, $P = .001$, 95% CI 1.008-1.034) (Table 4).

DISCUSSION

In this study, the α_1 angle and the α_1/α_2 ratio were evaluated as CTPA-derived continuous metrics to quantify RV geometric remodeling in response to acute pressure overload in patients with PE. Unlike conventional unidimensional parameters, these metrics simultaneously capture RV cavity expansion and leftward displacement of the interventricular septum as a single angular measurement, thereby providing a geometric representation of biventricular interdependence at the apical level. Both metrics remained independent predictors of in-hospital mortality after adjustment for the PESI. In contrast, the RV/LV diameter ratio did not provide incremental prognostic value beyond PESI when apical angle metrics were included in the model. Conversely, only PESI independently predicted long-term mortality, underscoring the distinction between acute geometric distortion and long-term disease trajectory.

The prognostic limitations of conventional CTPA parameters in acute PE are well established.[1-3,6-14] Although the RV/LV diameter ratio is widely used as a surrogate of RV pressure overload, its prognostic performance has shown considerable variability across studies. This may reflect the inherent limitation of unidimensional measurements, which fail to capture the integrated nature of RV expansion and septal deviation during acute pressure overload. In contrast, apical angle–based metrics incorporate both RV expansion and septal deviation within a single geometric construct, providing a more comprehensive representation of ventricular interdependence under acute pressure stress.[6-14,28]

Table 4. Cox Proportional Hazards Models for Long-Term All-cause Mortality

Variables	HR (Univariable)	HR (Multivariable)	*P* (Multivariable)
TAPSE at discharge (cm)	0.342 (0.141-0.812)	0.453 (0.182-1.094)	.076
RV/LV ratio at discharge	12.223 (1.143-131.162)	4.301 (0.358-51.664)	.251
PESI	1.021 (1.008-1.034)	1.021 (1.008-1.034)	.001
α_1 angle (degrees)	1.053 (0.962-1.144)	1.022 (0.941-1.113)	.650

α_1, right ventricular apical angle; HR, hazard ratio; PESI, pulmonary embolism severity index; RV/LV, right ventricle–to–left ventricle ratio; TAPSE, tricuspid annular plane systolic excursion.

Recent studies have explored alternative CT-derived geometric markers to better characterize RV remodeling. The ventricular septal curvature ratio has demonstrated strong predictive value for early clinical deterioration in normotensive PE patients.[23] The findings complement this work by demonstrating that apical angle metrics independently predict in-hospital mortality across the full clinical risk spectrum, including both normotensive and hemodynamically unstable patients. Importantly, whereas septal curvature indices require dedicated measurement of septal contour geometry, and volumetric RV/LV ratios necessitate advanced post-processing or reconstruction, α_1 and α_1/α_2 can be measured directly on routine axial CTPA images using standard angle tools, representing a practical advantage in time-sensitive clinical settings.[29] Furthermore, the α_1/α_2 ratio simultaneously encodes RV distension and LV compression as a dimensionless index, making it a simple and interpretable marker of biventricular geometric interaction.[30]

The associations observed between α_1 and echocardiographic markers of RV dysfunction further support the physiological validity of these metrics. In this cohort, α_1 demonstrated positive correlations with PASP and TR severity, and an inverse correlation with the TAPSE/PASP ratio. This pattern is consistent with prior studies demonstrating that the TAPSE/PASP ratio independently predicts in-hospital mortality in acute PE beyond clinical risk status and conventional imaging parameters.[26] The inverse relationship between α_1 and TAPSE/PASP suggests that progressive apical geometric deformation reflects not only structural RV cavity distortion but also functional impairment of RV–PA coupling. This mechanistic link may partly explain the independent mortality signal observed for α_1 beyond PESI. Taken together, CTPA-derived apical angle metrics and echocardiographic coupling indices appear to provide complementary, rather than redundant, insights into the hemodynamic consequences of acute RV pressure overload.[15-26,31,32]

From a pathophysiological perspective, the prognostic relevance of apical angle metrics can be understood within the framework of ventricular interdependence. Acute RV pressure overload leads to leftward deviation of the interventricular septum, increased RV free-wall stress, and progressive distortion of the RV cavity. This mechanical cascade directly impairs LV filling and systemic hemodynamics by reducing LV preload and constraining diastolic expansion.[6-14,28,30] At the apical level, this process manifests as widening of the RV apical angle and reciprocal narrowing of the LV apical angle, quantitatively captured by the α_1/α_2 ratio as a continuous geometric expression of biventricular interaction. The consistent associations observed in this study between α_1 and pulmonary arterial obstruction burden, RV–PA coupling indices, TR grade, and clinical risk status support the interpretation that apical geometric deformation is a sensitive marker of the hemodynamic severity of acute RV pressure overload. Whether advanced techniques such as 3-dimensional strain or apical rotational mechanics provide additional mechanistic insight beyond these geometric measures remains an open question for future research.

Despite significant improvements in RV overload parameters across all tertiles following treatment, patients with the most pronounced baseline apical distortion continued to exhibit incomplete early reverse remodeling at hospital discharge. In these patients, RV/LV and RA/LA diameter ratios remained higher, while TAPSE and S′ values remained lower compared with lower tertiles. Although treatment allocation was not randomized, the persistence of this pattern despite comparable or even more aggressive reperfusion strategies suggests that baseline geometric distortion may carry independent pathophysiological significance. These findings further indicate that the degree of initial geometric distortion may be associated with the extent and pace of RV structural recovery, independent of treatment modality, and support the concept that baseline geometric distortion may represent a structural "memory" of acute RV stress.[33-40] This observation has important clinical implications for early post-discharge risk stratification. Accordingly, patients presenting with markedly elevated α_1 values may warrant closer hemodynamic and imaging follow-up during the early post-discharge period, even after apparent clinical stabilization.

In contrast, neither α_1 nor the α_1/α_2 ratio was independently associated with long-term all-cause mortality after adjustment for PESI, for which only PESI retained independent predictive value. This finding supports the interpretation that apical angle–based metrics primarily reflect acute and potentially reversible geometric remodeling under sudden pressure overload, rather than the chronic disease burden that governs long-term prognosis. Rapid reverse remodeling following successful treatment likely attenuates the long-term prognostic relevance of baseline geometric alterations. Notably, Kaplan–Meier analysis demonstrated an early separation of survival curves across α_1 tertiles that did not reach conventional statistical significance—a borderline finding that may reflect limited statistical power rather than the absence of a true association. Prospective studies incorporating systematic longitudinal imaging are needed to clarify the long-term prognostic implications of apical geometric remodeling in acute PE.

Limitations

Several limitations of the present study should be acknowledged. First, the single-center, retrospective, observational design inherently carries the risk of selection bias, incomplete data capture, and measurement error. Nevertheless, the inclusion of consecutive patients and the use of predefined diagnostic and risk stratification algorithms may have partially mitigated these sources of bias. Second, measurements of α_1 and the α_1/α_2 ratio were derived from standard axial CTPA images, and technical variations in acquisition protocols, respiratory phase, heart rate, and reconstruction parameters may have contributed to measurement variability. Although all measurements were initially obtained by a single experienced observer, a reproducibility study conducted on a random validation subset of 50 patients yielded excellent inter-observer agreement, confirming that these CTPA-derived metrics are robust and objective. Nevertheless, multi-center validation across different centers, scanners, and software platforms remains to be

established. A relatively limited number of outcome events constrained the number of covariates that could be included in multiple models; parsimonious models were therefore intentionally applied to minimize overfitting, which may have limited the ability to explore the influence of additional potential confounders in greater detail. Analysis of LV rotational mechanics—including apical torsion and twisting—as well as 3-dimensional strain and strain rate analysis of both ventricles, might have provided more comprehensive mechanistic information. Finally, apical angle measurements were obtained exclusively from baseline CTPA studies at presentation, and the absence of serial imaging after hospital discharge precluded re-assessment of RV reverse remodeling beyond the in-hospital period, which may partly explain the lack of an independent association between α_1 or the α_1/α_2 ratio and long-term mortality.

CONCLUSION

This study identifies α_1 and the α_1/α_2 ratio as novel CTPA-derived markers that provide a quantitative assessment of acute right ventricular structural deformation in the setting of pulmonary embolism. These apical metrics offer significant incremental prognostic value beyond the conventional PESI score for the prediction of in-hospital mortality, reflecting their sensitivity to acute hemodynamic stress. However, as the PESI score remained the sole independent predictor of long-term survival, the clinical utility of these tomographic parameters is primarily centered on acute risk stratification during the hospital stay. These findings suggest that while apical remodeling is a robust indicator of short-term adverse outcomes, further prospective validation is required to define its role in comprehensive clinical management protocols.

Ethics Committee Approval: This study was approved by the Ethics Committee of Kartal Koşuyolu Heart and Research Hospital (Approval No: 2026/05/1399, Date: March 10, 2026).

Informed Consent: Informed consent was waived due to the retrospective nature of the study.

Peer-review: Externally peer-reviewed.

Author Contributions: Concept – B.K., C.K.; Design – B.K., C.K., Y.C.E., B.E.Ö.; Supervision – C.K., N.Ö., Ş.K.; Resources – B.K., C.K., Ç.E.Ç., A.H.; Materials – B.K., S.T.Ü., H.C.T., Ç.B., D.Ş.; Data Collection and/or Processing – S.T.Ü., H.C.T., Ç.B., D.Ş., İ.A., A.K., O.D., Ö.D.E., M.B.; Analysis and/or Interpretation – B.K., B.Keskin, A.H., Ş.K., C.K.; Literature Search – B.K., Y.C.E., B.E.Ö., S.T.Ü.; Writing – B.K., C.K.; Critical Review – B.K., C.K., Y.C.E., B.E.Ö., S.T.Ü., H.C.T., Ç.E.Ç., B.Keskin, Ç.B., D.Ş., İ.A., A.K., O.D., Ö.D.E., M.B., A.H., Ş.K., N.Ö.

Declaration of Interests: The authors have no conflict of interest to declare.

Funding: The authors declared that this study has received no financial support.

REFERENCES

1. Konstantinides SV, Torbicki A, Agnelli G, et al. 2014 ESC Guidelines on the diagnosis and management of acute pulmonary embolism. *Eur Heart J*. 2014;35(43):3033-3080. [CrossRef]
2. Piazza G. Advanced management of intermediate- and high-risk pulmonary embolism: JACC focus seminar. *J Am Coll Cardiol*. 2020;76(18):2117-2127. [CrossRef]
3. Konstantinides SV, Meyer G, Becattini C, et al. 2019 ESC Guidelines for the diagnosis and management of acute pulmonary embolism developed in collaboration with the European Respiratory Society (ERS). *Eur Heart J*. 2020;41(4):543-603. [CrossRef]
4. Leidi A, Bex S, Righini M, Berner A, Grosgurin O, Marti C. Risk stratification in patients with acute pulmonary embolism: current evidence and perspectives. *J Clin Med*. 2022;11(9):2533. [CrossRef]
5. Türkday Derebey S, Tokgöz HC, Keskin B, et al. A new index for the prediction of in-hospital mortality in patients with acute pulmonary embolism: the modified shock index. *Anatol J Cardiol*. 2023;27(5):282-289. [CrossRef]
6. Becattini C, Agnelli G, Germini F, Vedovati MC. Computed tomography to assess risk of death in acute pulmonary embolism: a meta-analysis. *Eur Respir J*. 2014;43(6):1678-1690. [CrossRef]
7. Meinel FG, Nance JW, Schoepf UJ, et al. Predictive value of computed tomography in acute pulmonary embolism: systematic review and meta-analysis. *Am J Med*. 2015;128(7):747-59.e2. [CrossRef]
8. Jia D, Zhou XM, Hou G. Estimation of right ventricular dysfunction by computed tomography pulmonary angiography: a valuable adjunct for evaluating the severity of acute pulmonary embolism. *J Thromb Thrombolysis*. 2017;43(2):271-278. [CrossRef]
9. Foley RW, Glenn-Cox S, Rossdale J, et al. Automated calculation of the right ventricle to left ventricle ratio on CT for the risk stratification of patients with acute pulmonary embolism. *Eur Radiol*. 2021;31(8):6013-6020. [CrossRef]
10. Samaranayake CB, Craigie M, Kempny A, et al. Right heart strain assessment on CTPA following acute pulmonary embolism: interobserver variability between expert radiologists and physicians. *Respir Med*. 2022;200:106928. [CrossRef]
11. Zantonelli G, Cozzi D, Bindi A, et al. Acute pulmonary embolism: prognostic role of computed tomography pulmonary angiography (CTPA). *Tomography*. 2022;8(1):529-539. [CrossRef]
12. Qanadli SD, El Hajjam M, Vieillard-Baron A, et al. New CT index to quantify arterial obstruction in pulmonary embolism: comparison with angiographic index and echocardiography. *AJR Am J Roentgenol*. 2001;176(6):1415-1420. [CrossRef]
13. Hu J, Tian X, Liu X, Ma G, Li C. Right ventricular area predicts short-term mortality in acute pulmonary embolism based on CT pulmonary angiography: a retrospective study. *Medicine*. 2023;102(10):e33116. [CrossRef]
14. Barco S, Mahmoudpour SH, Planquette B, Sanchez O, Konstantinides SV, Meyer G. Prognostic value of right ventricular dysfunction or elevated cardiac biomarkers in patients with low-risk pulmonary embolism: a systematic review and meta-analysis. *Eur Heart J*. 2019;40(11):902-910. [CrossRef]
15. Rudski LG, Lai WW, Afilalo J, et al. Guidelines for the echocardiographic assessment of the right heart in adults: a report from the American Society of Echocardiography endorsed by the European Association of Echocardiography, a registered branch of the European Society of Cardiology, and the Canadian Society of Echocardiography. *J Am Soc Echocardiogr*. 2010;23(7):685-713; quiz 786. [CrossRef]
16. Galderisi M, Cosyns B, Edvardsen T, et al. Standardization of adult transthoracic echocardiography reporting in agreement with recent chamber quantification, diastolic function, and heart valve disease recommendations: an expert consensus document of the European Association of Cardiovascular Imaging. *Eur Heart J Cardiovasc Imaging*. 2017;18(12):1301-1310. [CrossRef]

17. Mukherjee M, Rudski LG, Addetia K, et al. Guidelines for the echocardiographic assessment of the right heart in adults and special considerations in pulmonary hypertension: recommendations from the American Society of Echocardiography. *J Am Soc Echocardiogr*. 2025;38(3):141-186. [CrossRef]
18. Frémont B, Pacouret G, Jacobi D, Puglisi R, Charbonnier B, de Labriolle A. Prognostic value of echocardiographic right/left ventricular end-diastolic diameter ratio in patients with acute pulmonary embolism: results from a monocenter registry of 1,416 patients. *Chest*. 2008;133(2):358-362. [CrossRef]
19. Coutance G, Cauderlier E, Ehtisham J, Hamon M, Hamon M. The prognostic value of markers of right ventricular dysfunction in pulmonary embolism: a meta-analysis. *Crit Care*. 2011;15(2):R103. [CrossRef]
20. Pruszczyk P, Goliszek S, Lichodziejewska B, et al. Prognostic value of echocardiography in normotensive patients with acute pulmonary embolism. *JACC Cardiovasc Imaging*. 2014;7(6):553-560. [CrossRef]
21. Chornenki NLJ, Poorzargar K, Shanjer M, et al. Detection of right ventricular dysfunction in acute pulmonary embolism by computed tomography or echocardiography: a systematic review and meta-analysis. *J Thromb Haemost*. 2021;19(10):2504-2513. [CrossRef]
22. Wang D, Fan G, Zhang X, et al. Prevalence of long-term right ventricular dysfunction after acute pulmonary embolism: a systematic review and meta-analysis. *EClinicalmedicine*. 2023;62:102153. [CrossRef]
23. Gao Y, Gu Z, Wei X, et al. Ventricular septum curvature ratio: a novel imaging marker to predict clinical deterioration in normotensive acute pulmonary embolism. *Crit Care*. 2025;29(1):463. [CrossRef]
24. Keskin B, Tokgöz HC, Akbal ÖY, et al. Clinical, imaging and hemodynamic correlates and prognostic impact of syncope in acute pulmonary embolism: a single-center study. *Turk Gogus Kalp Damar Cerrahisi Derg*. 2022;30(3):317-326. [CrossRef]
25. Keskin B, Karagoz A, Hakgor A, et al. A novel method for the evaluation of right ventricular dysfunction in acute pulmonary embolism: myocardial work indices. *J Clin Ultrasound*. 2024;52(7):857-865. [CrossRef]
26. Kültürsay B, Keskin B, Tanyeri S, et al. Prognostic impact of the tricuspid annular plane systolic excursion/pulmonary arterial systolic pressure ratio in acute pulmonary embolism. *Anatol J Cardiol*. 2024;28(10):479-485. [CrossRef]
27. SCHULMAN S, KEARON C, Subcommittee on Control of Anticoagulation of the Scientific and Standardization Committee of the International Society on Thrombosis and Haemostasis. Definition of major bleeding in clinical investigations of antihemostatic medicinal products in non-surgical patients. *J Thromb Haemost*. 2005;3(4):692-694. [CrossRef]
28. Hakgör A, Tokgöz Demircan HC, Keskin B, et al. A novel composed index to evaluate the right ventricle free-wall adaptation against ventricular wall stress in acute pulmonary embolism. *Anatol J Cardiol*. 2023;27(7):423-431. [CrossRef]
29. Yucal A, Sayhan MB. Novel method for pulmonary embolism prognosis: right to left ventricular volume ratio (RLVR) on pulmonary angiography (CTPA). *Thromb Update*. 2025;19:100203. [CrossRef]
30. Alban F, André F, Mokry T, Erbel C, Frey N, Schell R. Mechanical thrombectomy improves left ventricular filling in intermediate-high risk pulmonary embolism: the role of ventricular interdependence. *Clin Res Cardiol*. 2026. [CrossRef]
31. Furlan A, Aghayev A, Chang C-CH, et al. Short-term mortality in acute pulmonary embolism: clot burden and signs of right heart dysfunction at CT pulmonary angiography. *Radiology*. 2012;265(1):283-293. [CrossRef]
32. Bikdeli B, Lobo JL, Jiménez D, et al. Early use of echocardiography in patients with acute pulmonary embolism: findings from the RIETE registry. *J Am Heart Assoc*. 2018;7(17):e009042. [CrossRef]
33. Kültürsay B, Tanyeri S, Keskin B, et al. Effectiveness and safety of reduced-dose and slow-infusion intravenous tissue-type plasminogen activator regimen in patients with acute pulmonary embolism at intermediate-high risk. *Anatol J Cardiol*. 2025;29(12):715-722. [CrossRef]
34. Kaymaz C, Akbal OY, Tanboga IH, et al. Ultrasound-assisted catheter-directed thrombolysis in high-risk and intermediate-high-risk pulmonary embolism: a meta-analysis. *Curr Vasc Pharmacol*. 2018;16(2):179-189. [CrossRef]
35. Kaymaz C, Akbal OY, Keskin B, et al. An eight-year, single-center experience on ultrasound assisted thrombolysis with moderate-dose, slow-infusion regimen in pulmonary embolism. *Curr Vasc Pharmacol*. 2022;20(4):370-378. [CrossRef]
36. Kültürsay B, Keskin B, Tanyeri S, et al. Ultrasound-assisted catheter-directed thrombolytic therapy vs. anticoagulation in acute intermediate-high risk pulmonary embolism: a quasi-experimental study. *Anatol J Cardiol*. 2025;29(6):312-320. [CrossRef]
37. Akbal ÖY, Keskin B, Tokgöz HC, et al. A seven-year single-center experience on AngioJet rheolytic thrombectomy in patients with pulmonary embolism at high risk and intermediate-high risk. *Anatol J Cardiol*. 2021;25(12):902-911. [CrossRef]
38. Kaymaz C, Kültürsay B, Tokgöz HC, et al. Is it time to reappraise for black-box warning on AngioJet rheolytic thrombectomy in patients with pulmonary embolism: a systematic review and meta-analysis. *Anatol J Cardiol*. 2024;28(6):264-272. [CrossRef]
39. Kaymaz C, Tokgöz HC, Kültürsay B, et al. Current insights for catheter-directed therapies in acute pulmonary embolism: systematic review and our single-center experience. *Anatol J Cardiol*. 2023;27(10):557-566f. [CrossRef]
40. Kultursay B, Kaymaz C, Tokgoz HC, et al. From clusters to outcomes: machine learning-based phenotyping in intermediate–high-risk acute pulmonary embolism. *Pulm Circ*. 2026;16(1):e70243. [CrossRef]

SUPPLEMENTARY MATERIAL

Standardized Measurement Protocol for Apical Angles

To ensure reproducibility, apical angles (α_1 and α_2) were measured using a three-step standardized process:

1. **Slice Selection:** Measurements were performed on the axial CT slice demonstrating the maximal transverse dimension of the RV cavity and where all four cardiac chambers were best visualized simultaneously.
2. **Apex Definition:** The RV apex was defined as the most distal point of the RV endocardial contour. The LV apex was defined as the corresponding most distal point of the LV endocardial contour on the same or adjacent slice showing the maximal LV longitudinal axis.
3. **Annular Landmarks:** The medial landmark for the tricuspid annulus was the insertion point of the septal leaflet at the interventricular septum, and the lateral landmark was the junction of the RV free wall and the tricuspid valve plane. For the mitral valve, the medial and lateral insertion points of the mitral leaflets were used.
4. **Angle Construction:**

α_1: One line followed the interventricular septum's endocardial contour (RV side), and the other followed the RV free wall contour, both originating from the RV apex and extending to the respective tricuspid annular landmarks.

α_2: Two lines followed the LV endocardial contours from the LV apex to the mitral annular edges.

Supplementary Table 1. Incremental Prognostic Value of CTPA-Derived Apical Metrics Over the PESI Score

Model	Continuous NRI (95% CI)	*P*	IDI (95% CI)	*P*
Baseline Model (PESI Score)	Reference	-	Reference	-
Model A (PESI + α_1)	0.474 (-0.073 to 1.021)	0.089	0.027 (-0.008 to 0.062)	0.134
Model B (PESI + α_1/α_2)	0.778 (0.270 to 1.286)	0.002	0.016 (0.001 to 0.032)	0.034

Abbreviations: NRI, Net Reclassification Improvement; IDI, Integrated Discrimination Improvement; PESI, Pulmonary Embolism Severity Index; α_1, Right ventricular apical angle; α_1/α_2, Ratio of right-to-left ventricular apical angles.

Supplementary Table 2. Multivariable Logistic Regression Analysis Adjusted for Treatment Modality as Sensitivity Analysis

Predictor Variable	Coefficient (β)	Standard Error	z-value	*P*
Model S1: α_1 based				
Intercept	-11.567	2.462	-4.698	< 0.001
PESI Score	0.028	0.007	4.145	< 0.001
α_1	0.144	0.063	2.307	0.021
CDT	-0.757	0.69	-1.097	0.273
Model S2: α_1/α_2 based				
Intercept	-9.73	1.806	-5.387	< 0.001
PESI Score	0.029	0.007	4.125	< 0.001
α_1/α_2 ratio	2.491	1.136	2.193	0.028
CDT	-0.824	0.692	-1.19	0.234

Abbreviations: CDT, Catheter-direceted treatment; NRI, Net Reclassification Improvement; IDI, Integrated Discrimination Improvement; PESI, Pulmonary Embolism Severity Index; α_1, Right ventricular apical angle; α_1/α_2, Ratio of right-to-left ventricular apical angles.

Supplementary Table 3. Incremental Predictive Value of CT-derived Apical Metrics Beyond the PESI Score

Model Comparison	Continuous NRI	*P*	IDI	*P*
PESI + α_1/α_2 ratio vs. PESI	0.778	0.002	0.016	0.034
PESI + α_1 vs. PESI	0.474	0.089	0.027	0.134

Abbreviations: NRI, Net Reclassification Improvement; IDI, Integrated Discrimination Improvement; PESI, Pulmonary Embolism Severity Index; α_1, Right ventricular apical angle; α_1/α_2, Ratio of right-to-left ventricular apical angles.

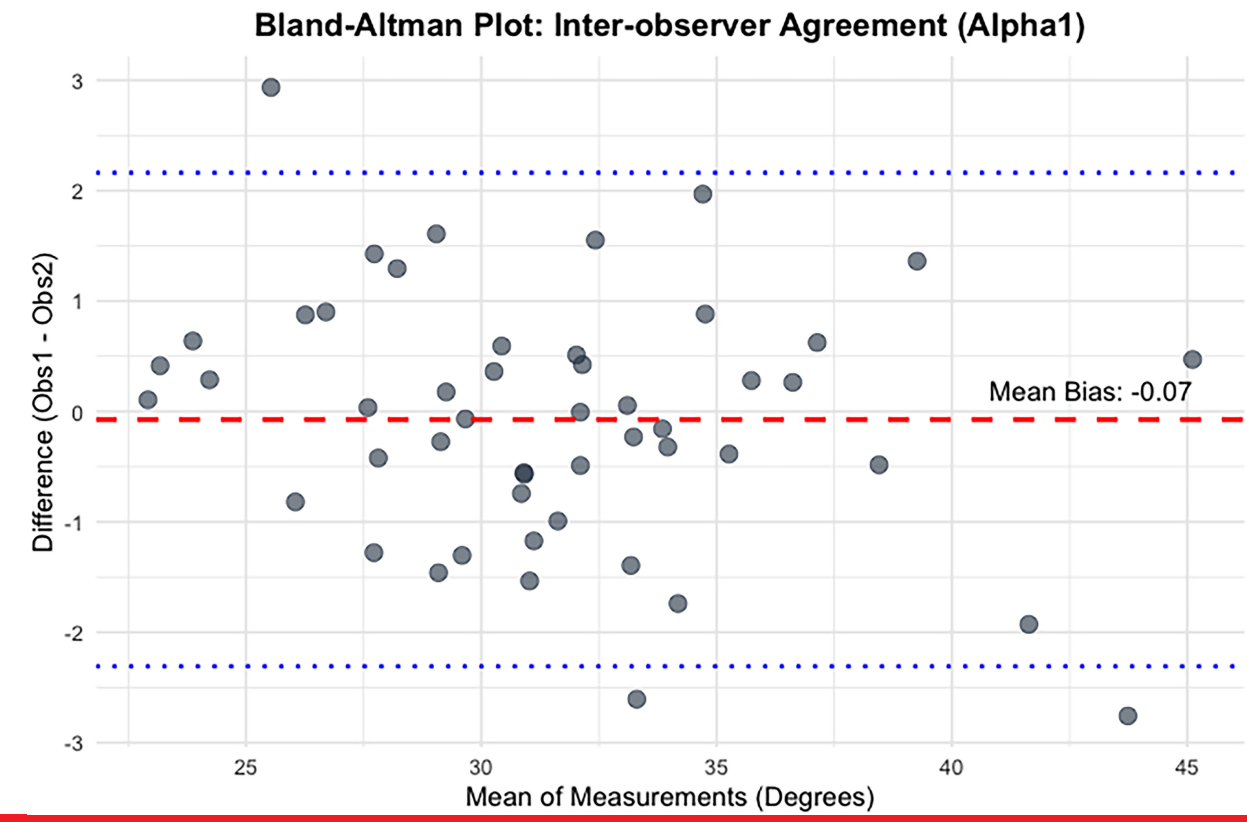

Supplementary Figure 1. Bland-Altman Plot for Inter-Observer Agreement of Right Ventricular Apical Angle (α1) Measurements.

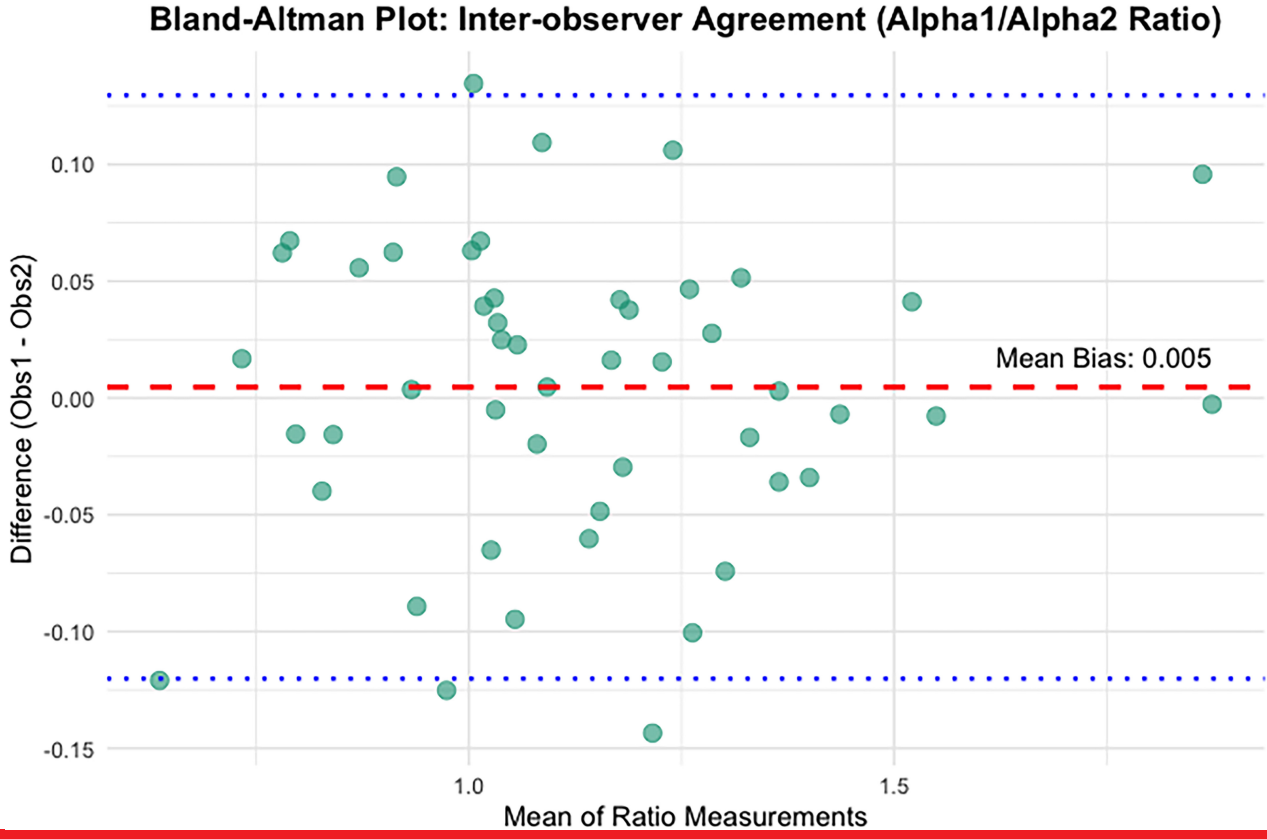

Supplementary Figure 2. Bland-Altman Plot for Inter-Observer Agreement of the Right-to-Left Ventricular Apical Angle Ratio (α1/α2) Measurements.

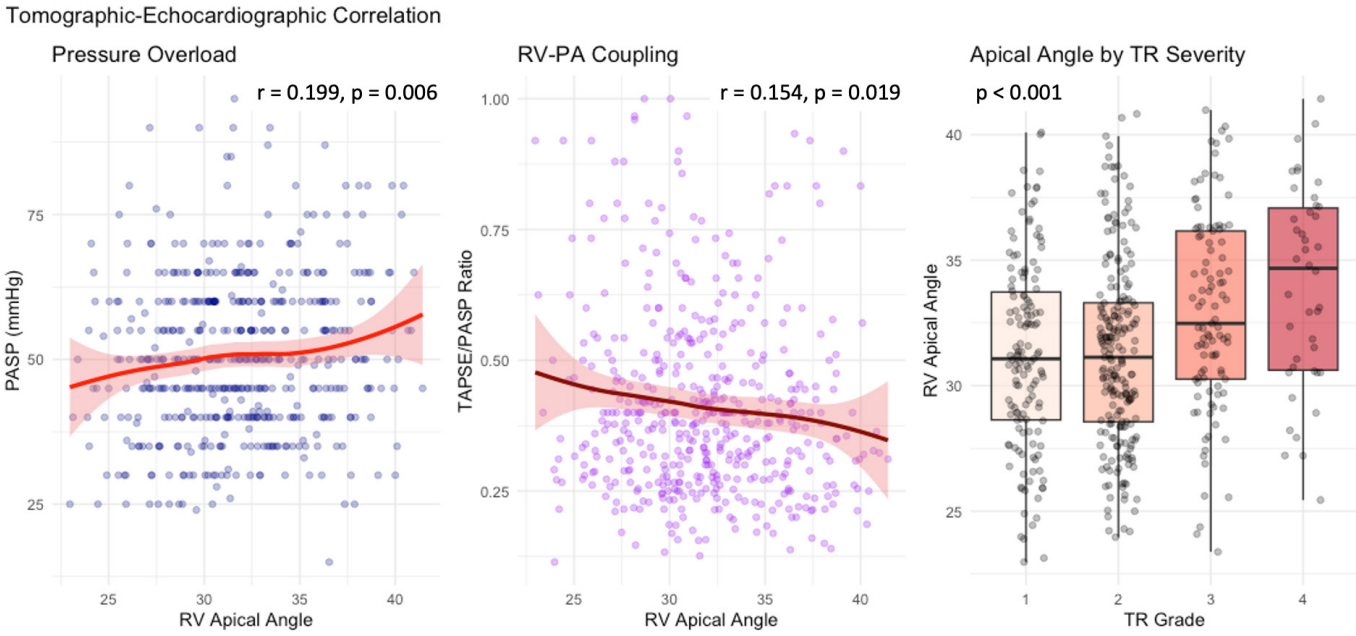

Supplementary Figure 3 Tomographic-Echocardiographic Correlates of Right Ventricular Apical Angle (α1).